

# Determination and Optimization of the Contact Pattern of Worm Gears

Bernd-Robert Höhn, Karl Steingröver and Michael Lutz

## Summary

The load capacity of worm gears is mainly influenced by the size and the position of the contact pattern. A new method was developed that allows for the determination and optimization of the idle and load contact patterns in the design stage. By this method, the contours of worm and worm wheel are simulated point by point, taking into account the boundary conditions of the manufacturing process.

The idle contact pattern can be derived from these contours by pairing them together in such a way that the assembly deviations define the position of worm and wheel. The load contact pattern can be determined from the idle contact pattern by adding the deflections of the teeth and gear bodies and the elastic deformations of the bearings and the housing.

This procedure can also be used for automated optimization of the contact pattern, so optimum machine settings can be found without a trial manufacturing. Comparisons of these theoretical contact patterns with real contact patterns of gears in practice showed a good correlation.

## Introduction

The load capacity of worm gear drives is mainly influenced by the size and the position of the contact pattern. The actual load capacity calculations according to DIN 3996 (Ref. 1) or ISO CD 14521 (Ref. 2) assume contact patterns that are well positioned and cover nearly the whole flank of the wheel.

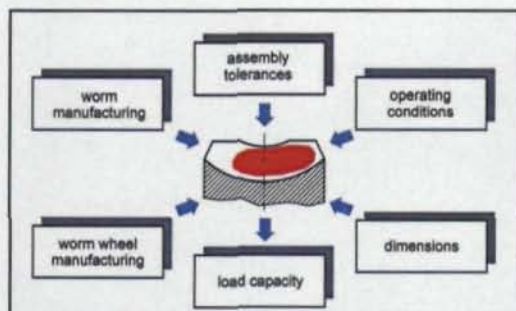


Figure 1—Influence parameters on the contact pattern of worm gears.

Size and position of the contact pattern depend on many parameters, like manufacturing type, accuracy, geometry of the housing, kind of bearings and operating conditions (see Fig. 1).

The estimation of the influence of these parameters on the contact pattern, and therefore on the load capacity, requires great experience.

Normally, the idle contact pattern is checked after assembly by painting some teeth of the wheel with contact paint. After several revolutions, the abrasion of the contact paint is used to evaluate the idle contact pattern. Although this procedure is simple, it is time consuming. Furthermore, experience is needed if the contact pattern has to be adjusted. Other disadvantages of this method are that the load contact pattern and local specific overloads cannot be detected. To avoid this old-fashioned procedure, an analytical method was developed that allows for the determination of the idle and load contact patterns in the design stage.

These investigations were carried out at the Gear Research Centre (FZG) at the Technical University of Munich, Germany, and were supported by the Gear Research Organization (FVA) of Frankfurt, Germany, through research project 252 (Ref. 3).

## Idle Contact Pattern

By this new method, the contours of the worm and the wheel are calculated point by point by taking into account the boundary conditions and deviations of the manufacturing process.

The points of the worm in the axial sections and the wheel in the corresponding sections are described by simulating the final manufacturing process (grinding wheel or hob). Then, these two contours are brought into contact in a way so the center distance and the assembly deviations define the position of each contour. If this is done for several mesh positions, the idle contact pattern is then the summation of the smallest distances between the contours of worm and wheel at each mesh position.

**Calculation of the contour of the worm.** The contour of different types of worm flanks can be described by simulating the final manufacturing process, which is usually done by grinding or cutting. In accord with DIN 3975, the worm's flank contours that are ground include a concave profile in the axial section, an involute profile in the transverse section and a convex profile in the axial section. The flank contours that are cut include a straight profile in the axial section and a straight profile in the normal section (Ref. 4). The grinding disk, for example, can be characterized by the diameter  $d_0$ , the pressure angle  $\alpha_0$  and the profile (see Figure 2).

The contour of the grinding disk can be either described by analytical equations (Ref. 5) or approximated by a series of discrete points. Here the approximation by discrete points is used.

The discrete points of the worm contour can be achieved from the points of the grinding disk by simulating the manufacturing process in a way so the grinding disk has to be rotated around the worm axis in several steps and simultaneously has to be moved in the direction of the worm axis to achieve the lead. An example is shown in Figure 3.

The advantage of this procedure over the analytical method is that the real geometry—which deviates from the ideal geometry—can be taken into account. These deviations are grinding with a modified center distance, modified pressure angle or modified lead. Furthermore, modifications like crowning can be added to this model.

**Calculation of the contour of the worm wheel.** The basic idea for calculating the contour of worm wheel flanks is the same as shown for the worm. Here the final manufacturing process is usually done by cutting. The hob can be characterized by the diameter  $d_0$ , the pressure angle  $\alpha_0$  and the profile.

The hob's contour can also be approximated by a series of discrete points. The discrete points of the wheel contour can be achieved by simulating the manufacturing process as shown in Figure 4. Here the hob has to be rotated around the wheel axis in several steps and simultaneously moved in the feed direction. An example for such a wheel tooth contour is shown in Figure 5.

Because the contour of the wheel is not based on empirical equations, the influences of modifications on the hob, like increased hob diameter, center distance modification and lead modification, can be taken into account.

**Simulation of the assembly of the worm gear.** During the assembly of worm and wheel in the

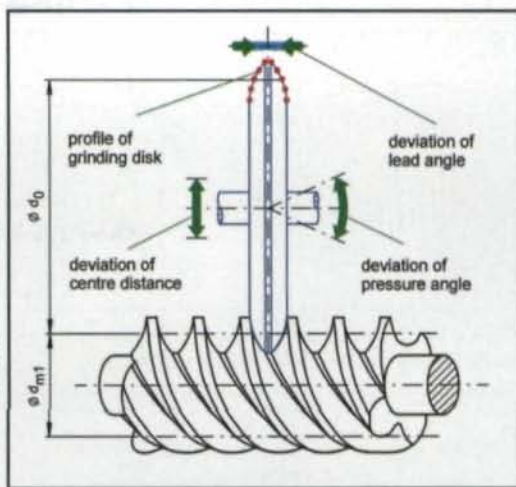


Figure 2—Derivation of the worm contour by simulating the grinding process.

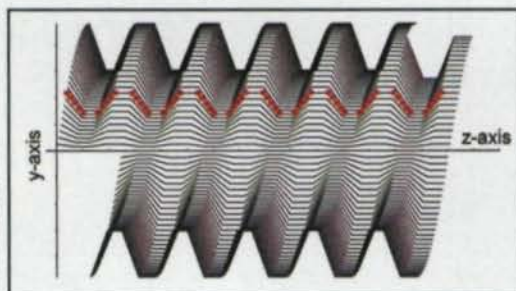


Figure 3—Contour of a worm with a straight profile in the axial section and with two teeth (individual points only shown for one plane).

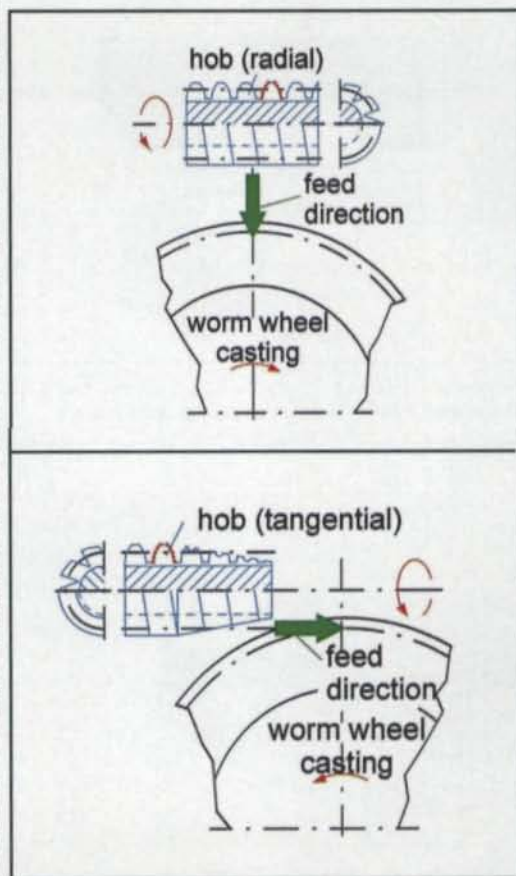


Figure 4—Derivation of the worm wheel contour by simulating the cutting process (radial or tangential).

### Prof. Dr.-Ing. Bernd-Robert Höhn

is head of the Gear Research Centre, a part of the Technical University of Munich, located in Germany. The centre's main activities include theoretical and experimental investigations of spur, helical, bevel and worm gears and development of software for calculating geometry and load capacity of gears.

### Dr.-Ing. Karl Steingröver

is a chief engineer at the Gear Research Centre and is responsible for its worm gear and computer programming groups.

### Dr.-Ing. Michael Lutz

is a distributor of gear and chain drives via his company, Ingenieurservice Lutz GmbH of Altdorf, Germany. Previously, he worked in the Gear Research Centre's worm gear group and carried out the investigations described in this paper.

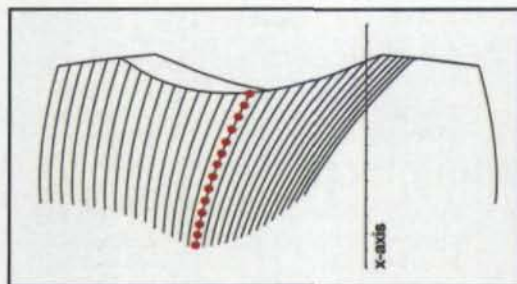


Figure 5—Contour of one tooth of a worm wheel (individual points only shown in one plane).

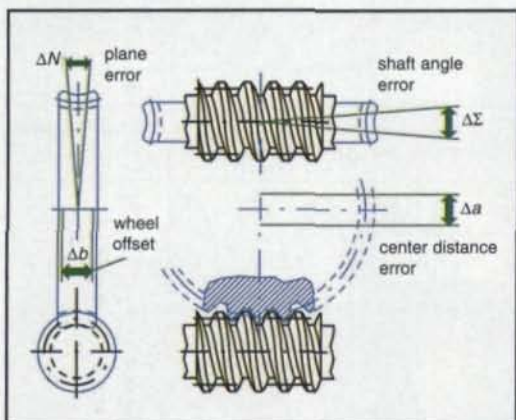


Figure 6—Deviations from the ideal mounting position of worm and wheel in the housing.

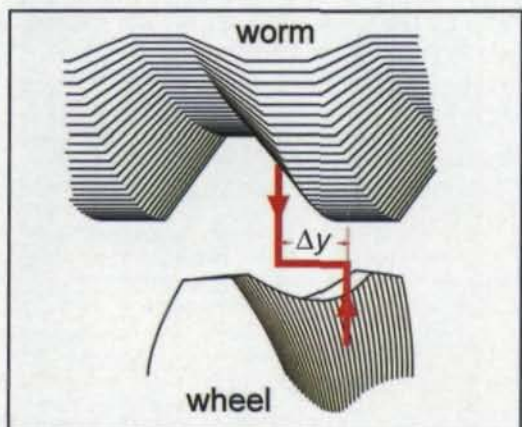


Figure 7—Pairing of the contours of the teeth of worm and wheel (individual points not shown).

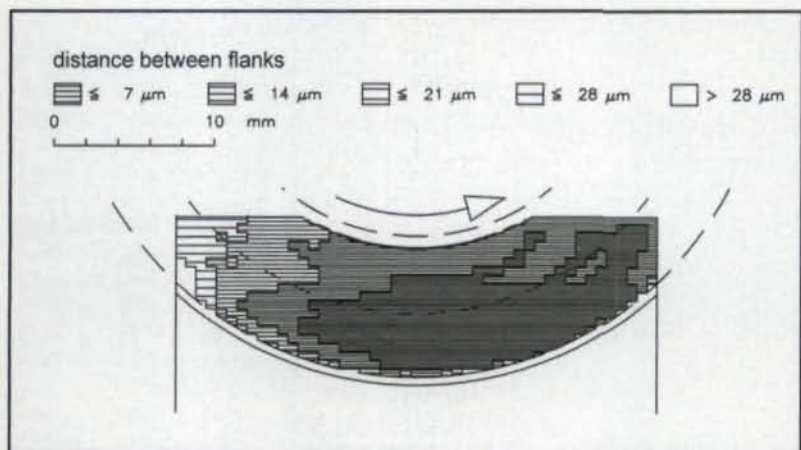


Figure 8—Example for an idle contact pattern.

housing, deviations from their ideal position can occur. These deviations, of course, also have an influence on the size and the position of the contact pattern. The most important deviations are (see Fig. 6):

- wheel offset  $\Delta b$ ,
- deviation of the center distance  $\Delta a$ ,
- shaft angle error  $\Delta\Sigma$ , and
- plane error  $\Delta N$ .

If the contour from the discrete points of the worm and wheel teeth are known, the assembly process can then be simulated by sliding the worm and wheel together, taking into account the aforementioned boundary conditions.

Now the distances between the different points of worm and wheel can be calculated. Usually for one pair of points there is a minimum distance  $\Delta y_0$  (see Figure 7). From all distances  $\Delta y_i$ ,  $\Delta y_0$  has to be subtracted. Distances, which fall into a specified small range, can now be viewed as contact points for this position of worm and wheel. These contact points form one contact line. This procedure has to be repeated for a series of positions of worm and wheel. The individual contact lines then form the idle contact pattern. An example is shown in Figure 8.

#### Load Contact Pattern and Specific Load

The idle contact pattern is not identical to the load contact pattern. Under load, the contact pattern is further influenced by the worm deflection, the tooth deflection, deflection of the gear bodies and the elastic deformations of the bearings and the housing. For the determination of the load contact pattern and the specific load, the method of influence numbers is used. In this model, all influences that do not depend on the load are described by a rigid body, while all load-dependent influences are described by a spring system (see Fig. 9). The application of a tooth load to this model leads to deformations at the different stiffnesses and therefore to different specific loads at the specific points along the flank. The load contact pattern is the summation of all points where the load is  $> 0$ .

For load-free conditions and ideal geometries, the pads (spring system) and the wedges (rigid body) are in contact over the whole length (see Fig. 9a). This is the theoretical contact line. For real geometries with no load, there is a contact only in one point (see Fig. 9b). In this position, the pad is still undeformed. These are the boundary conditions of the idle contact pattern. Under load, the pads will be deformed (see Fig. 9c). The total

deformation can be described by a system of equations. For the determination of the discrete deformations at each contact point and the determination of the single loads at these points, the following equations have to be solved:

Summation of the single loads:

$$F_{bn} = \sum F_i = E \cdot F \quad (1)$$

with:  $F_{bn}$  = total load,  $F_i$  = single load in a spring element,  $E$  = unit vector, and  $F$  = vector with all single loads.

Components of a single deformation:

$$\delta_i^* = \delta_{ges} - \delta_i \quad (2)$$

with:  $\delta_i^*$  = single deformation in one spring element,  $\delta_{ges}$  = total deformation of the pad, and  $\delta_i$  = distance between spring element and pad with no load.

System of load-deformation equations:

$$\delta^* = q \cdot F \quad (3)$$

with:  $\delta^*$  = vector with single deformations and  $q$  = matrix with all elastic components.

These equations lead to Equation 4:

$$F_{bn} = E \cdot q^{-1} \cdot [\delta_{ges} - \delta_i] \quad (4)$$

This is a scalar equation, where  $F_{bn}$  is known from the torque. The determination of the matrix  $q$  with all elastic components is made by calculating all influences separately according to Equation 5:

$$q = q^{SW} + q^{SZ} + q^{RW} + q^{RZ} + q^{WL} + q^{GH} \quad (5)$$

where the single matrices with elastic components are (see Fig. 10):

$q^{SW}$  for the influence of worm shaft deflection,

$q^{SZ}$  for the influence of the deflection of a thread of the worm,

$q^{RW}$  for the influence of the wheel shaft deflection,

$q^{RZ}$  for the influence of the deflection of a tooth of the wheel,

$q^{WL}$  for the influence of the deformation of the bearings, and

$q^{GH}$  for the influence of the deformation of the housing.

The determination of the different matrices can be done by using the method of influence numbers. This is shown as an example for the deformation of a tooth of the wheel (see Fig. 11).

To determine the influence numbers for the tooth deformation, the theory of thin slices is used. For each contact point, one slice is used. Depending on the tooth shape and the point where the load acts, the deviation of the tooth can be cal-

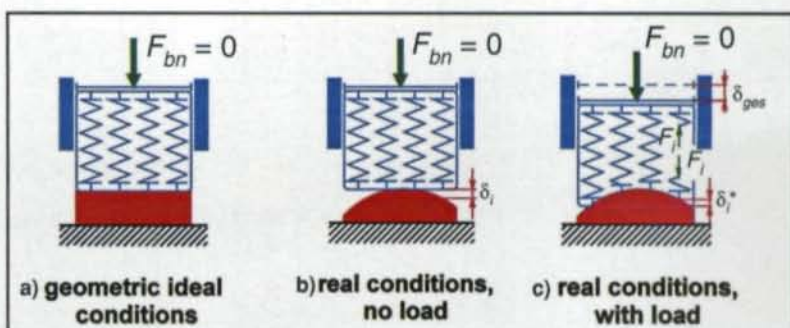


Figure 9—Model of the mesh between worm and worm wheel: a) geometric ideal conditions; b) real conditions, no load; c) real conditions, with load.

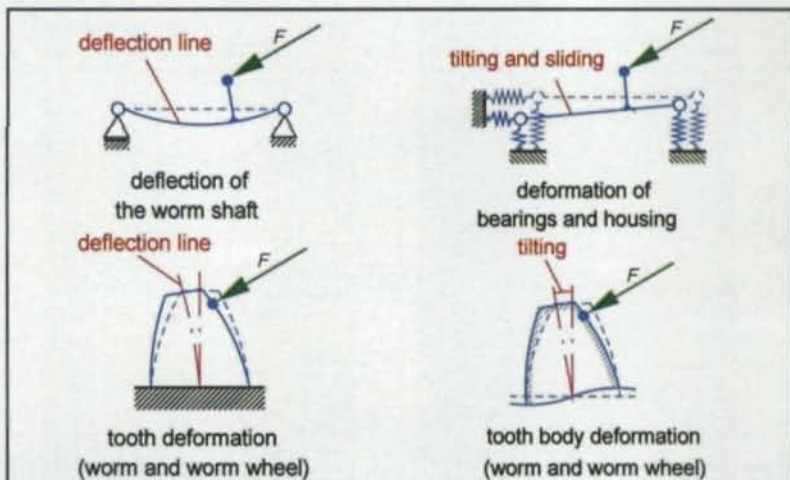


Figure 10—Mechanical models for determination of the matrix with elastic components.

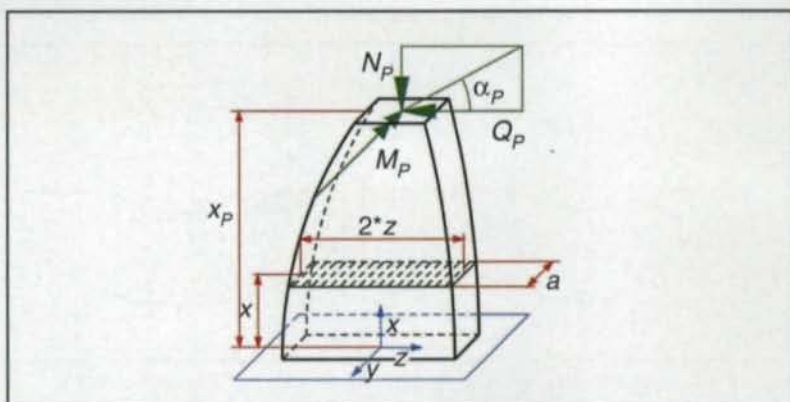


Figure 11—Slice model for the influence of the deformation of a tooth of a wheel; thickness  $a$  = constant.

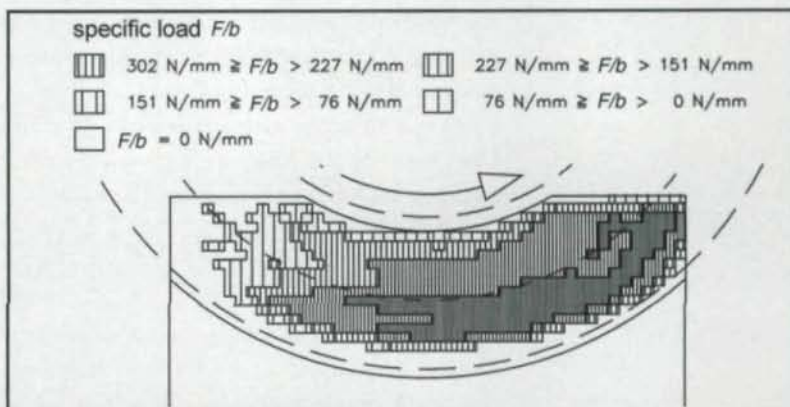


Figure 12—Example of a load contact pattern

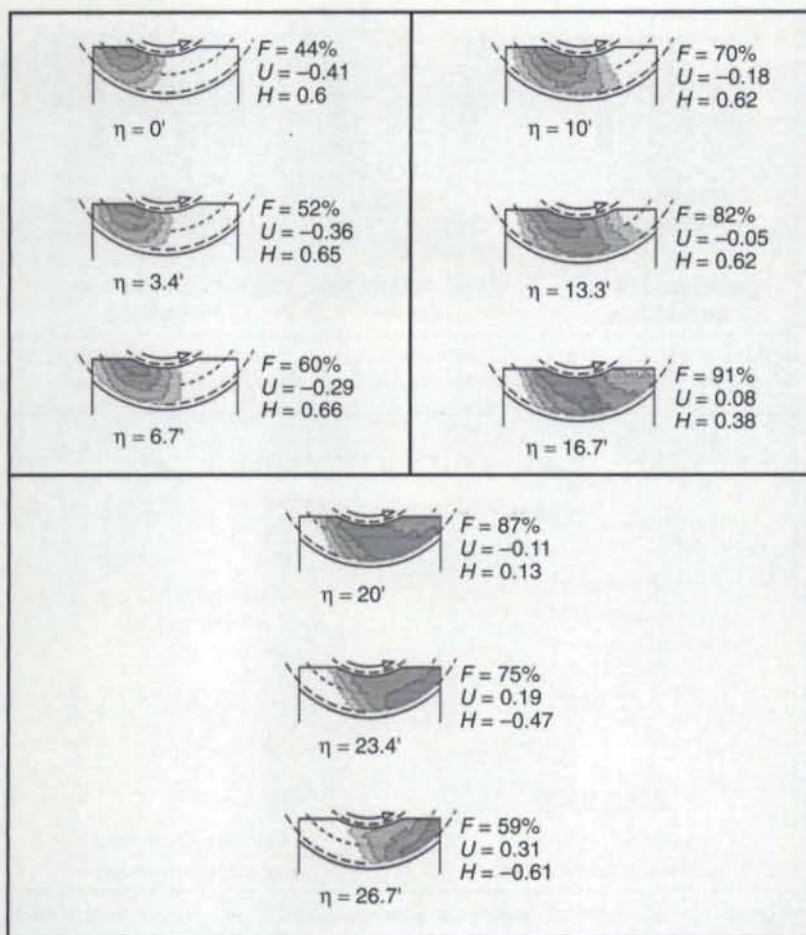


Figure 13—Series of contact patterns depending on the traverse angle of the hob.

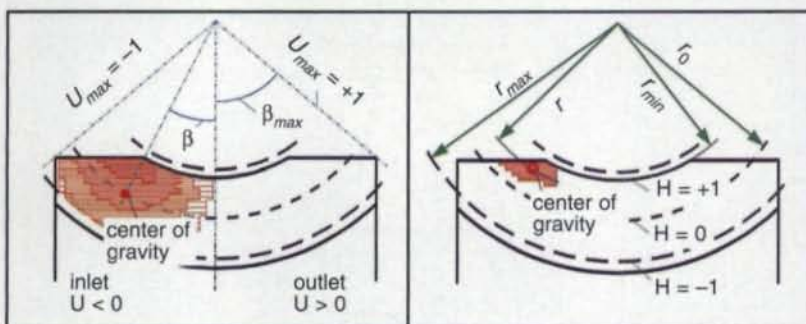


Figure 14—Specification of contact pattern according to size and position.

culated according to the theory of Weber and Banaschek (Ref. 6). The load  $P$  is divided into its components:  $Q_p$ ,  $N_p$  and  $M_p$ . These lead to a normal load  $N$ , a transverse load  $Q$  and a bending moment  $M$  in the section at  $x$ .

To determine the deformation in the direction of the load, the deformation energy is set equal to the integral over the elastic stress energy. It is:

$$\frac{1}{2} P w_z = \frac{1}{2} \int_0^{\alpha_p} \frac{M^2}{EI} dx + \frac{1}{2} \int_0^{\alpha_p} \frac{Q^2}{GA_s} dx + \frac{1}{2} \int_0^{\alpha_p} \frac{N^2}{EA} dx \quad (6)$$

with:  $P$  = load,  $w_z$  = deformation in direction of the load,  $x_p$  = length of the slice,  $\alpha_p$  = load direction angle,  $Q$  = transverse load at  $x$ ,  $N$  = normal load at  $x$ ,  $M$  = bending moment at  $x$ ,  $E$  = Young's

modulus,  $G$  = shear modulus,  $I$  = mass moment of inertia at  $x$ ,  $A$  = cross section at  $x$ , and  $A_s$  = shear area at  $x$ .

This equation can be solved in the direction of the deformation  $w_z$ , which can be viewed as one point in the matrix  $q^{RZ}$ .

The result of this procedure is a load contact pattern as shown in Figure 12. Contrary to the idle contact pattern, where the different levels characterize the minimum distances between worm and wheel, the different levels of the load contact pattern characterize the specific loads along the contact lines.

#### Optimization of the Contact Pattern

The procedures described in the previous sections lead to contact patterns that correspond very well with measured contact patterns of gears in practice. Normally, the measured contact patterns do not have the optimum size and position. Therefore, an optimization must be done, for which great experience is necessary. A contact pattern, calculated by using the procedures described in the previous sections, can be optimized by variation of the different manufacturing and assembly parameters. This makes sense only if there is knowledge of how the different parameters influence the size and position of the contact pattern. In the following, a procedure is described stating how this selection can be done automatically.

First, the parameters—which can be varied for achieving a better contact pattern—have to be selected. Then, a series of calculations has to be made by varying these parameters in several small steps. This leads to a series of contact patterns. An example of such a series is shown in Figure 13.

From this series, the optimum contact pattern (and the corresponding manufacturing and assembly parameters) can be found by classifying the size and position of the contact patterns using the characterizing parameters  $F$ ,  $U$  and  $H$ :

The parameter  $F$  is the calculated area of the contact pattern as a percentage of the theoretical possible contact area as shown in the left part of Figure 14.

The parameter  $U$  characterizes the position of the contact pattern in the circumferential direction of the worm. For the calculation of  $U$ , the center of gravity of the area used for the determination of  $F$ , is used (see left part of Fig. 14). It can be determined using Equation 7:

$$U = \pm \beta/\beta_{max} \quad (7)$$

Per definition, values for  $U$  between  $-1$  and  $+1$  are possible. If the center of gravity is in the inlet area,  $U$  will have a negative value;  $U = 0$  if the center of gravity is in the middle of the flank and a position in the outlet area has a positive value.

The parameter  $H$  describes the position of the contact pattern in the direction of the tooth height. For this, the center of gravity of that area of the contact pattern is used where the smallest distances were calculated in the case of the idle contact pattern or the highest specific loads were calculated in the case of the load contact pattern. (see right part of Fig. 14). The restriction on this small area was done because if the whole area is used, contact patterns with peaks at the tip or the root would be classified as well-adjusted contact patterns.  $H$  can be determined as follows:

$$H = (r - r_{min})/(r_0 - r_{min}) \text{ if } r < r_0$$

$$H = (r - r_{min})/(r_0 - r_{max}) \text{ if } r \geq r_0 \quad (8)$$

Also, the parameter  $H$  can reach values between  $-1$  and  $+1$ , where a positive value represents a position of the contact pattern in the direction of the tip of the tooth and a negative value represents a position in the direction of the root.

The result of this classification is shown by an example in Figure 15. A typical position of a contact pattern is in the tooth height direction in the middle and in the circumferential direction tending slightly into the outlet area. This means  $H$  should be in the area of  $0$  and  $U$  should be in the area of  $0.1$ . In the example, this corresponds to a traverse angle  $\eta \approx 20^\circ$ , which leads to a size of the contact pattern (parameter  $F$ ) of  $87\%$ .

### Conclusion

These procedures were verified by a comparison of calculated idle contact patterns with real contact patterns of worm gears in practice. An example from this comparison is shown in Figure 16. From this figure, it can be seen that the calculated contact pattern correlates very well with the measured contact pattern. Therefore, these procedures are suitable for the determination and optimization of the contact pattern of worm gears.  $\odot$

This paper was previously presented at the International Conference on Gears, held March 13–15, 2002, in Munich, Germany. Also, the paper was previously published by VDI Verlag in the conference's proceedings, in VDI report 1665.

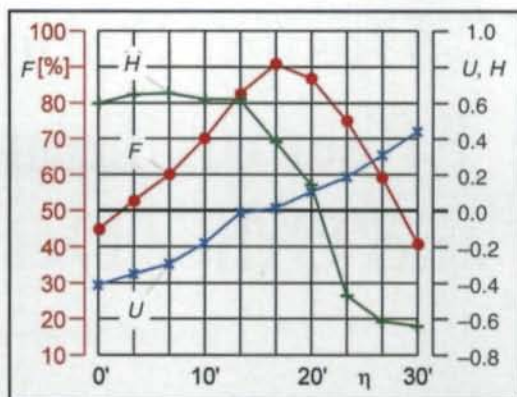


Figure 15—Results of the classification of the calculated contact patterns (example).

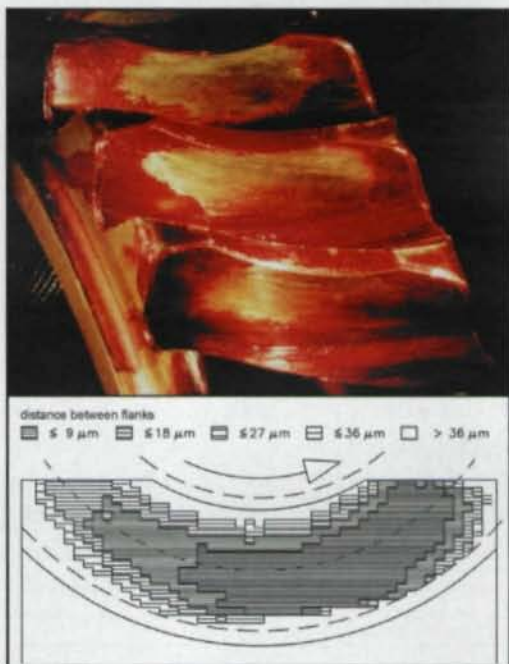


Figure 16—Comparison of a real contact pattern with the calculated contact pattern.

### References

1. Deutsches Institut für Normung e.V. "DIN 3996—Tragfähigkeitsberechnung von Zylinder-Schneckengetrieben mit Achsenwinkel  $\Sigma = 90^\circ$ ," Beuth Verlag, Berlin, Germany, 1998.
2. International Organization of Standardization, "ISO CD 14521—Load Capacity Calculation of Worm Gears," 2001.
3. Lutz, M. "Berechnungsprogramm zur Ermittlung des Tragbildes zwischen Schnecke und Schneckenrad," FVA-Forschungsvorhaben No. 252, Forschungsvereinigung Antriebstechnik e.V., Issue 500, Frankfurt, Germany, 1996.
4. Deutsches Institut für Normung e.V., "DIN 3975—Begriffe und Bestimmungsgrößen für Zylinderschneckengetriebe mit sich rechtwinklig kreuzenden Achsen," Beuth Verlag, Berlin, Germany, 2001.
5. Niemann, G. and H. Winter. *Maschinenelemente Band III*, Springer Verlag, Berlin, Germany, 1986.
6. Weber, C. and K. Banaschek. *Formänderung und Profilrücknahme bei gerad- und schrägverzahnten Rädern*, Vieweg-Verlag, Schriftenreihe Antriebstechnik 11, Braunschweig, Germany, 1955.

Tell Us What You Think . . .

Visit [www.geartechnology.com](http://www.geartechnology.com) to

- Rate this article
- Request more information
- Contact the authors or organization mentioned
- Make a suggestion

Or call (847) 437-6604 to talk to one of our editors!